InP-based Complementary HBT Amplifiers for use in Communication Systems

Donald Sawdai and Dimitris Pavlidis

Solid-State Electronics Laboratory
Department of Electrical Engineering and Computer Science
The University of Michigan, Ann Arbor, Michigan 48109, U.S.A.
http://www.eecs.umich.edu/dp-group/

Abstract— This paper addresses a method to improve the linearity characteristics of power amplifiers by developing a PNP HBT technology and combining the PNP HBTs with NPN HBTs in a push-pull amplifier. InP-based PNP HBTs were fabricated with $h_{fe} > 30$, $BV_{ECO} = 5.6$, and f_T and f_{max} of 11 and 31 GHz, respectively, which is the best reported for InAlAs/InGaAs PNP HBTs.

Common-collector push-pull amplifiers were simulated using these HBTs, demonstrating an improvement of 14 dB in second harmonic content under Class B operation. A common-emitter push-pull amplifier fabricated with the same HBTs demonstrated the best IM3 (by ~7 dBc) and smaller second harmonic content (by ~9 dBc) compared with NPN HBTs. In addition, the circuit produced 1.32 dBm more output power than the NPN HBT alone at 1 dB of gain compression.

This work was supported by ARO MURI under Contract DAAH04-96-1-0001.

I. Introduction

Wireless communication systems require power amplifiers with high linearity, high power-added efficiency (PAE), and high power-handling capability. HBTs offer this capability, and AlGaAs/GaAs devices have already been introduced in wireless systems. Another promising device approach is InP-based HBTs, which have demonstrated very good high-frequency performance and have been implemented in various integrated circuits for electronic and optoelectronic applications. Their power capability is promising, with power levels up to 1.4 mW/μm^2 reported by the authors using NPN single HBT designs [1]. Further enhancement is possible by means of double heterojunction designs, and a power density of 3.6 mW/μm^2 with PAE of 54% at 9 GHz has been reported with the latter approach from Hughes Research Labs [2]. InP/InGaAs HBTs are consequently of interest for power amplification in communication systems.

This paper addresses another method to improve power performance by developing a PNP HBT technology and combining the PNP HBTs with NPN HBTs in a push-pull amplifier. While not as impressive as their NPN counterparts, the current state-of-the-art performance for PNP HBTs is sufficient for applications up to X-band, and further enhancement in capability can be achieved. The best-published InAlAs/InGaAs PNP HBTs demonstrated $\beta = 30$, $f_T = 13$ GHz, and $f_{max} = 35$ GHz as reported by the authors [3], while the best-published InP/InGaAs PNP HBTs were reported by AT&T with $\beta = 20$, $f_T = 11$ GHz, and $f_{max} = 25$ GHz [4].

Complementary push-pull amplifiers have several advantages over single-transistor power amplifiers, and they are much simpler to design than NPN-only push-pull amplifiers. Since the output voltage swing is generated across two transistors in the push-pull amplifier,

approximately twice the output voltage is possible. In addition, push-pull amplifiers can produce linear output in Class AB or Class B, which can have efficiencies as high as 78%. To achieve the same linearity, single transistor amplifiers must operate in Class A, with efficiency limited to 50%. InP-based HBTs offer an additional advantage for push-pull operation: the turn-on voltage V_{BE} is approximately 0.75 V, versus 1.4 V for GaAs-based HBTs. This smaller turn-on voltage reduces both crossover distortion and overall power consumption.

In this paper, we present issues and results on complementary push-pull circuits fabricated in the InP material system. A first report on such circuits was recently presented by the authors [5]. This paper provides further details on their design and performance. First, device results are presented for both the NPN and the PNP HBTs used in this study. Then, simulations of complementary amplifiers are presented to demonstrate the advantages of push-pull amplifiers. Finally, the results from a hybrid common-emitter push-pull amplifier are presented and discussed.

II. Integration of NPN and PNP HBTs

Several technologies are available for integrating NPN and PNP HBTs in order to fabricate circuits. In the InAlAs/InGaAs material system, first PNP and then NPN HBT layers have been grown uninterrupted on a mesa-patterned substrate, which resulted in a planar wafer with NPN and PNP HBTs after device fabrication [6]. In addition, several NPN/PNP integration technologies have been demonstrated in the AlGaAs/GaAs material system. Hybrid common-emitter push-pull amplifiers using $6f\times2\times20$ μm^2 HBTs have demonstrated 6 dB of gain, 0.5 W of output power, and 42% PAE at 10 GHz [7]. Selective low-pressure OMVPE has also been used to create monolithic common-emitter push-pull amplifiers that demonstrate power combination

at 10 GHz with power cancellation in the second harmonic [8]. Finally, selective MBE has been used to monolithically create common-collector push-pull amplifiers that produce 7.2 dB gain and 7.5 dBm output power at 2.5 GHz using $4f \times 3 \times 10\ \mu m^2$ HBTs [9].

InP-based HBTs offer several advantages over GaAs-based HBTs in satisfying the requirements of wireless communications. In general, the improved frequency performance of InP-based HBTs produces higher gain at high frequencies. The lower contact and sheet resistances of the emitter cap and subcollector layers, along with the smaller offset voltage (0.2 V vs. 0.4 V), reduce the saturation "knee" voltage of InP-based HBTs and allow the use of low-voltage batteries. Since InP has ten times smaller surface recombination velocity than GaAs, the current gain is more uniform with bias, which should produce better amplifier linearity. Less surface recombination also increases the gain of large power HBTs with many emitter fingers (large total periphery), and it also allows for very small HBTs for digital applications. Finally, the higher thermal conductance of the InP substrate (0.7 W/cm-K, versus 0.5 for GaAs) allows for more power dissipation in any given HBT design. InP-based single HBTs do suffer from low breakdown voltages, typically around 2 to 7 V. This limitation can be overcome in double HBTs with InP collectors. An additional benefit of double HBTs is that the offset voltage is reduced to almost 0 V.

III. InP-based NPN and PNP HBT Performance

Both the NPN HBTs and the PNP HBTs used in this study were grown and fabricated on semi-insulating InP wafers at The University of Michigan. The NPN InP/InGaAs epilayers were grown using an EMCORE low-pressure Metalorganic Chemical Vapor Deposition system, while the PNP InAlAs/InGaAs epilayers were grown by solid-source Molecular Beam Epitaxy. The

HBTs were fabricated using our standard self-aligned processes, which produces a 0.2-μm base contact-to-emitter separation. The base-collector capacitance was minimized by using the base contact as a self-aligned etch mask for the base mesa. Electroplated gold airbridges were used to connect the HBTs to coplanar interconnect pads for off-wafer bonding or for on-wafer probing, and micro-trenches were wet-etched to isolate the semiconductor junctions under the airbridge pads from the intrinsic HBTs. Detailed HBT results from these NPN [1] and PNP [10] layers can be found elsewhere.

The HBTs used in this study had 5×10 μm^2 emitters. The NPN HBTs had a DC small-signal gain $h_{fe} > 70$. Their maximum collector current density was about $J_C = 1.4\times10^5$ A/cm^2, and the breakdown for large NPN HBTs was as high as $BV_{CE0} = 7.2$ V. Their optimal f_T and f_{max} were 97 GHz and 51 GHz, respectively, at $V_{CE} = 2.0$ V and $I_C = 46$ mA. Similarly, the PNP HBTs had a DC small-signal gain $h_{fe} > 30$. Although the maximum collector current density was about $J_C = 9\times10^4$ A/cm^2, the current gain compressed rapidly for $J_C > 5\times10^4$ A/cm^2. The breakdown for these HBTs was $BV_{EC0} = 5.6$ V at 10 A/cm^2. Microwave measurements resulted in optimal f_T and f_{max} of 11 GHz and 31 GHz, respectively, at $V_{EC} = 4.0$ V and $I_C = 11.7$ mA.

On-wafer power characterization was performed at 10 GHz using a system developed in-house with FOCUS electromechanical tuners on both the source and the load. The PNP HBTs were characterized using load pull techniques and demonstrated a small-signal gain of 10 dB, peak power-added-efficiency of 24%, and maximum output power density of 0.49 mW/μm^2 [10]. These characteristics are very similar to the NPN HBTs, which had slightly higher gain (+1dB) and efficiency (+5%) but produced less output power than the PNP HBTs (-3dBm). Also note

that these results are very similar to power performance published for PNP AlGaAs/GaAs HBTs [11]: $P_{out} = 0.57$ mW/μm^2 and $PAE = 33\%$ at 10 GHz.

Further studies of the PNP HBTs indicated that output power scaled linearly with the number of emitter fingers up to 10 fingers, which was the largest HBT measured. The microwave gain was constant up to 4 emitter fingers, and the gain degraded by 3 dB when the number of emitter fingers was increased to 10. Finally, common-base PNP HBTs provided 3 to 6 dB more gain than similarly biased common-emitter PNP HBTs, which resulted in 5% higher efficiency. These results confirmed the suitability of the PNP HBTs for high-frequency power applications.

IV. Push-pull Simulations and Issues

In order to investigate the benefits of using PNP HBTs together with NPN HBTs in various integrated circuits, the large-signal characteristics of several NPN-only and complementary amplifiers were simulated. For these simulations, non-linear large-signal models were extracted for the HBTs from the previous section. These extractions accurately reproduced most HBT characteristics that dominate the power, efficiency, and linearity performance, such as parasitic resistances and capacitances, turn-on voltage, saturation voltage, Early effect, gain non-uniformity with I_C, and base-collector breakdown. These large-signal HBT models were then used in all of the circuit simulations.

The fist circuit investigated was a Class B common-collector push-pull output stage (*Figure 1*) consisting of one NPN and one PNP HBT. DC blocking capacitors were used to allow for a single 5.6-V DC power supply to the circuit. The circuit was simulated using the non-linear HBT models in the time domain over a wide range of input power at 1.9 GHz. The

results were then compared to similar simulations of single NPN and PNP common-collector power amplifiers with the base unbiased for Class B operation. For the individual NPN and PNP amplifiers, the collector was biased through an RF choke to a single 1.8 V or -3.8 V supply, respectively, which gave optimal performance without HBT breakdown.

The input/output power characteristics of the Class B push-pull amplifier are shown together with those of the individual HBTs in *Figure 2*. Since the DC gain of the HBTs is low at very small bias, the microwave gain for the Class B amplifiers is low for small P_{in}. However, as P_{in} increases, self-biasing causes the DC I_C to increase, which in turn increases the microwave gain of the amplifier. The peak gain for the NPN and PNP amplifiers were 12.4 and 3.5 dB, respectively, with the push-pull gain at an intermediate 8.6 dB. For larger input power, the waveform peaks pushed the HBTs into saturation, limiting further output power. Note, however, that the maximum output power from the push-push circuit was roughly 3 dB more than from the individual HBTs, since at that point that output power from both saturated HBTs in the circuit are combined. Although its higher gain gave the NPN amplifier higher PAE at low P_{in}, the push-pull amplifier's higher saturated P_{out} allowed it to achieve that same peak PAE as the NPN amplifier of 40%. Note that these Class B circuits are off and consume no DC power when there is no input signal.

The advantage of the push-pull amplifier can be seen in the harmonic content of the signal from *Figure 2*. At the beginning of P_{out} saturation, the second harmonic content of the output of the NPN and PNP amplifiers are both -7 dBc. The theoretical even-order harmonic cancellation in the push-pull amplifier reduces its second harmonic content to -21 dBc. However, since the odd-order harmonics do not inherently cancel in push-pull amplifiers, its

third harmonic shows little variation from the NPN and PNP amplifiers at similar levels of self-biasing.

The second circuit investigated is a Class AB version of previous circuit, with two diode-connected HBTs between the bases of the amplifying NPN and PNP HBTs for biasing (see *Figure 3*). Two resistors and two inductors serve to bias these diodes. This Class AB push-pull amplifier was compared to Class AB single NPN and Class AB single PNP amplifiers, both which had the base biased by a similar two-resistor two-inductor network.

The input/output power characteristics of the Class AB push-pull amplifier are shown together with those of the individual HBTs in *Figure 4*. Since the Class AB amplifiers keep the HBTs slightly on even when no input signal is present, the low-gain region at low I_C is avoided, so that the microwave gain is almost flat for all P_{in} below output power saturation. This microwave gain, 10.3/13.0/6.8 dB for the push-pull/NPN/PNP amplifiers, is somewhat higher than for the Class B case. Otherwise, the gain of the Class AB amplifiers behave similar to their Class B counterparts. Even with no input signal present, the Class AB amplifiers draw significant DC power – for example, the push-pull circuit draws 13.0 mW through the bias network and 12.0 mW through the HBT pair. Therefore, the Class AB peak PAE, 36%, is slightly lower than that of the Class B amplifier. However, the PAE for $P_{in} < +3$ dBm is higher for the Class AB amplifier than for Class B due to its much higher gain.

The Class AB push-pull amplifier demonstrates second harmonic cancellation: -25 dBc at P_{out} saturation, versus -16 dBc for the NPN and PNP amplifiers. The third harmonic is also reduced from -20 dBc for the NPN and PNP amplifiers to -30 dBc for the push-pull amplifier at the same power levels. For the push-pull amplifier, the second harmonic content is slightly

reduced (-4 dB) when moving from Class B to Class AB, while the third harmonic content is greatly reduced (-14 dB) due to the elimination of the cross-over distortion.

Similarly, the Class AB circuit was also simulated using large-signal models derived from published characteristics of typical NPN and PNP AlGaAs/GaAs HBTs [12, 13, 14]. When using the same V_{CC} = 6.2 V, the peak gain of the GaAs-based circuit (7.7 dB) was 2.6 dB less than the InP-based circuit, primarily due to the better frequency performance of the InP NPN HBT. Both the larger turn-on voltage and the larger knee voltage of the GaAs HBTs limited the output power at 1 dB of gain compression to 12.7 dBm, which is 3.1 dB lower than for the InP push-pull circuit. This reduced P_{out}, together with increased power consumption due to the larger turn-on voltage, limited the GaAs-based PAE to 25%, as compared to the InP-based PAE of 36%. Although these results do not necessarily reflect the full potential of each technology, since they are based on typical rather than optimized characteristics, they do indicate the power advantages of InP-based HBTs over GaAs-based HBTs in push-pull amplifiers.

The InP-based simulations demonstrate several advantages of the push-pull amplifiers over single-HBT amplifiers. The main advantage is the reduced distortion due to harmonic cancellation, which ideally would show higher improvements if the NPN and PNP HBTs were better matched in terms of gain. Another advantage is the 3-dB increase in output power, which is primarily achievable due to the 5.6-V supply used in the push-pull amplifier. These NPN HBTs have BV_{CE0} = 7.2 V, but they degrade rapidly when conducting more than a few milliamps for V_{CE} > 3.0 V. While the push-pull creates up to 4 V of V_{CE} across the NPN HBT when the NPN is off and the PNP is on, the V_{CE} across the NPN is less than 2.5 V when the NPN is on.

The same argument also holds for the PNP, allowing the push-pull circuit a greater supply voltage without breakdown and hence greater output power than single-HBT amplifiers.

Both Class B and Class AB push-pull amplifiers had only moderate PAE when compared to the theoretical maximum of 78% for Class B. The primary limitation on PAE was the large knee voltage for the HBTs: 0.5 V and 2.1 V at I_C =30 mA for the NPN and PNP, respectively, which together reduced the available output voltage swing from the 5.6-V DC supply to 3.0 V. Reducing the collector and emitter parasitic resistances will reduce the knee voltage, especially for the PNP. Also, using a graded emitter-base junction or using a large bandgap collector can reduce the offset voltage, which would also reduce the knee voltage. The other limitation is the low gain at low I_C, which reduces the gain and linearity of the Class B amplifier. Enhanced emitter-base junction designs and fabrication technologies can increase the gain at low I_C, which would enable the Class B amplifier to improve its linearity and gain while maintaining its high PAE.

V. Push-pull Experiment

In order to verify the benefits of complementary technologies, a complementary common-emitter push-pull amplifier was designed and fabricated using the NPN and PNP HBTs described above. Although the common-collector amplifier with single bias supply described in the previous section would be used more often as a power amplifier in a real communication system, a common-emitter amplifier with four bias supplies was fabricated in this experiment. The common-emitter design is simpler for a first-run test, and it directly demonstrates the advantages of complementary amplifiers.

A passive coplanar circuit was designed and fabricated on 10-mil alumina substrates to permit feeding of NPN and PNP common-emitter HBTs from a common input signal probe (see *Figure 5*). The HBTs were thinned to 200 μm, cleaved, and then mounted in the circuits on the alumina substrates. Gold bond wires connected the HBT chips to the electroplated gold interconnects on the circuit. An X-band test bench was designed for a variety of on-wafer measurements on the push-pull amplifier.

The circuit characteristics were measured at 8 GHz with both NPN and PNP in Class A (I_{C0} = 20.3 mA and 11.6 mA, respectively). The input versus output power curves are shown in *Figure 6*, which also shows the power output at the second harmonic for single-tone excitation and the third-order intermodulation (IM3) power output for two-tone excitation at 500 kHz separation. Note that for the circuit, this graph shows the *total* power input to the circuit and *total* power output from the circuit; therefore, each HBT in the circuit is receiving half of the input power. The data for the individual HBTs were measured independently for each HBT. At 1 dB of gain compression, the NPN and PNP HBTs produced 7.7 and 7.5 dBm of output power, respectively, while the circuit produced 9.0 dBm. This ~1.4 dB increase in output power is limited by the gain mismatch between the NPN and the PNP HBTs; when the circuit is at 1-dB compression (P_{in} = +0.9 dBm), each HBT receives –2.1 dBm input power, causing the high-gain NPN to be over-saturated and the low-gain PNP to be under-saturated. If the HBTs were perfectly matched, both HBTs would produce the same gain and saturate at the same P_{in}, which would result in 3 dB increase in output power for the push-pull circuit. Note that the simulations do demonstrate the full 3 dB increase in output power, mainly due to the different bias scheme used there.

Figure 6 also demonstrates the improvements in linearity for the circuit when compared to the NPN HBT alone. At the highest power levels measured, the circuit demonstrated less IM3 (by ~7 dBc) and smaller second harmonic content (by ~9 dBc) when compared to the NPN HBT. These numbers indicate an advantage for the push-pull circuit even under Class A operation.

VI. Conclusions

In this paper, we present the characteristics of PNP InP-based HBTs, simulated results on complementary push-pull HBT amplifiers, and first results on the implementation of similar complementary HBT amplifiers. The PNP HBTs demonstrated 10 dB of gain and output power that scaled well with HBT area at 10 GHz. Both the simulations and experiments demonstrate an improvement to the linearity characteristics of NPN HBT amplifiers by including a PNP HBT in a push-pull configuration. Simulations also indicate that reducing the parasitic emitter and collector resistances can substantially improve the amplifier efficiency, and more advanced emitter-base junction designs can increase the gain and linearity of Class B amplifiers.

Such complementary amplifiers could lead to improved wireless communication systems. The high efficiency and Class B operation increases battery life, and the decreased harmonic distortion allow the use of popular modulation techniques with reduced signal bandwidth, such as QPSK. In addition, integration of NPN and PNP HBTs offers other benefits, such as higher gain and less power consumed in small-signal amplifier stages through the use of active loads.

Acknowledgments

The authors would like to thank Dr. K. Hong for the growth of the NPN HBT wafers and Dr. X. Zhang and Prof. P. Bhattacharya for the growth of the PNP HBT wafers.

References

[1] D. Sawdai, J-O Plouchart, D. Pavlidis, A. Samelis, and K. Hong, "Power Performance of InGaAs/InP Single HBTs," *8th Int. Conf. InP and Related Materials*, pp. 133-136, April 1996.

[2] C. Nguyen, T. Liu, M. Chen, and R. Virk, "Bandgap Engineered InP-Based Power Double Heterojunction Bipolar Transistors," *9th Int Conf Indium Phosphide and Related Materials*, pp. 15-19, 1997.

[3] D. Sawdai, X. Zhang, D. Pavlidis, and P. Bhattacharya, "Performance Optimization of PNP InAlAs/InGaAs HBTs," *Proc IEEE/Cornell Conf on Advanced Concepts in High Speed Semiconductor Devices and Circuits*, pp. 269-277, 1997.

[4] L. M. Lunardi, S. Chandrasekhar, and R. A. Hamm, "High-Speed, High-Current-Gain P-n-p InP/InGaAs Heterojunction Bipolar Transistors," *IEEE Electron Dev. Lett.*, Vol. 14, pp. 19-21, January 1993.

[5] D. Sawdai and D. Pavlidis, "Power Amplification using NPN and PNP InP HBTs and Application to Push-Pull Circuits," *22nd Workshop on Compound Semiconductor Devices and Integrated Circuits (WOCSDICE)*, pp. 45-46, 1998.

[6] W. Stanchina, R. Metzger, M. Pierce, J. Jensen, L. McCray, R. Wong-Quen, and F. Williams, "Monolithic Fabrication of NPN and PNP AlInAs/GaInAs HBTs," *5th Int. Conf. InP and Related Materials*, pp. 569-571, 1993.

[7] H. Tserng, D. Hill, T. Kim, "A 0.5-W Complementary AlGaAs-GaAs HBT Push-Pull Amplifier at 10 GHz," *IEEE MW & Guided Wave Lett.*, Vol. 3, No. 2, pp. 45-47, February 1993.

[8] D. Slater Jr., P. Enquist, and J. Hutchby, "Harmonic Canellation in Monolithic AlGaAs/GaAs Npn/Pnp HBT Push-Pull Paris," *Proc IEEE/Cornell Conf on Advanced Concepts in High Speed Semiconductor Devices and Circuits*, pp. 305-314, 1991.

[9] K. Kobayashi, D. Umemoto, J. Velebir, A. Oki, and D. Streit, "Integrated Complementary HBT Microwave Push-Pull and Darlington Amplifiers with p-n-p Active Loads," *IEEE J. Solid-State Circuits*, Vol. 28, No. 10, pp. 1011-1017, October 1993.

[10] D. Sawdai, X. Zhang, D. Pavlidis, and P. Bhattacharya, "Power Performance of PNP InAlAs/InGaAs HBTs," *10th Int. Conf. InP and Related Materials*, pp. 72-75, 1998.

[11] D. Hill, T.S. Kim, and H.Q. Tserng, "X-band Power AlGaAs/InGaAs P-n-p HBT's," *IEEE Electron Dev. Lett.*, Vol. 14, pp. 185-187, April 1993.

[12] D. Slater, P. Enquist, J. Hutchby, A. Morris, and R. Trew, "Pnp HBT with 66 GHz f_{max}," *IEEE Electron Dev. Lett.*, Vol. 15, pp. 91-93, March 1994.

[13] D. Umemoto, J. Velebir, K. Kobayashi, A. Oki, and D. Streit, "Integrated *npn/pnp* GaAs/AlGaAs HBTs Grown by Selective MBE," *Electronics Lett.*, Vol. 27, pp. 1517-1518, August 15 1991.

[14] D. Hill, T. Kill, H. Tserng, "AlGaAs/GaAs Pnp HBT with 54 GHz F_{max} and Application to High-Performance Complementary Technology," *51st Ann. Device Research Conf.*, Paper IIIA-6, 1993.

Figure Captions

Figure 1: Circuit diagram of Class B push-pull amplifier with single bias supply used in simulations.

Figure 2: Simulated power output at fundamental, second, and third harmonics for Class B push-pull, NPN-only, and PNP-only amplifiers at 1.9 GHz.

Figure 3: Circuit diagram of Class AB push-pull amplifier used in simulations.

Figure 4: Simulated power output at fundamental, second, and third harmonics for Class AB push-pull, NPN-only, and PNP-only amplifiers at 1.9 GHz.

Figure 5: Micrograph of fabricated NPN/PNP push-pull common-emitter amplifier.

Figure 6: Measured power output at fundamental, second harmonic, and third-order intermodulation for NPN HBT, PNP HBT, and push-pull amplifier at 8 GHz.

Figures

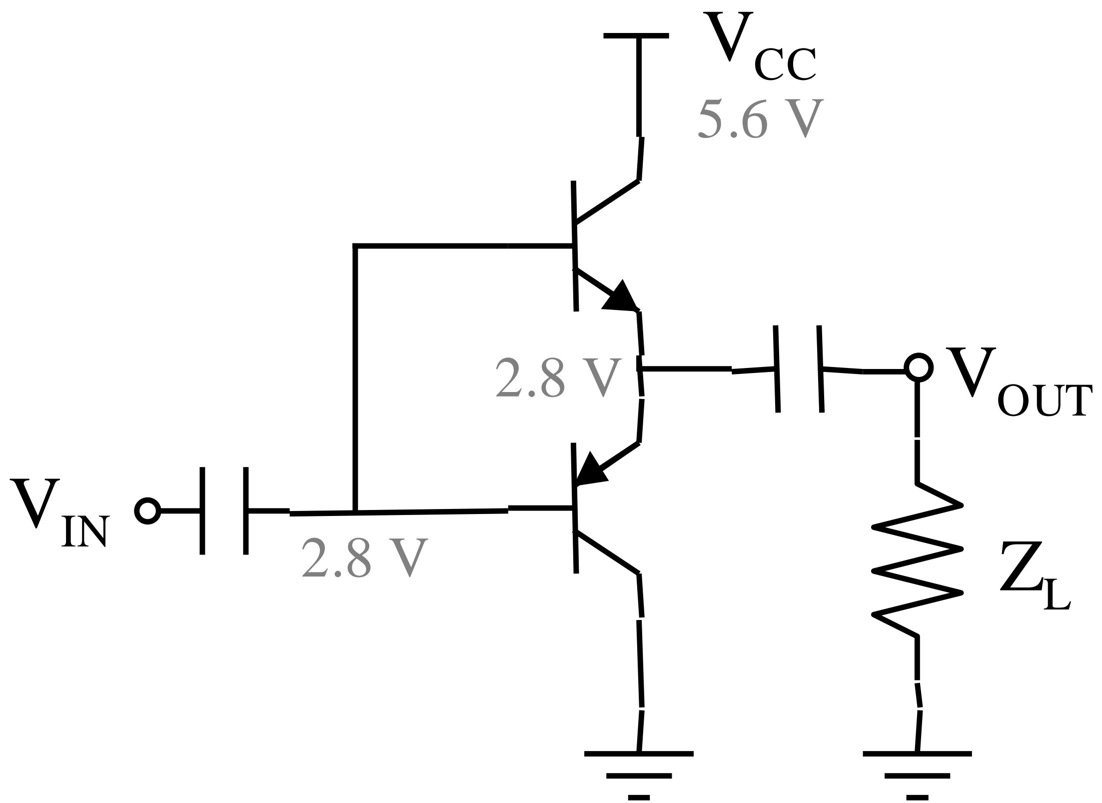

Figure 1

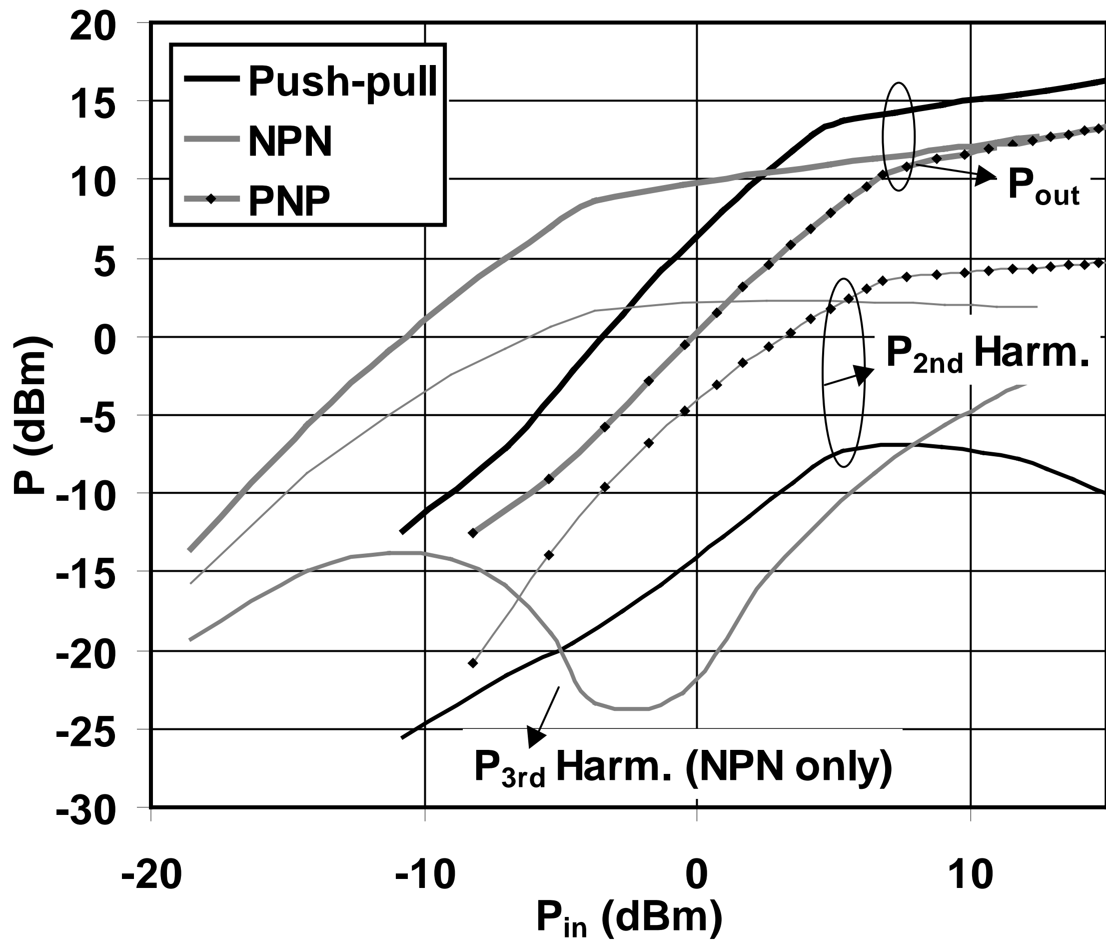

Figure 2

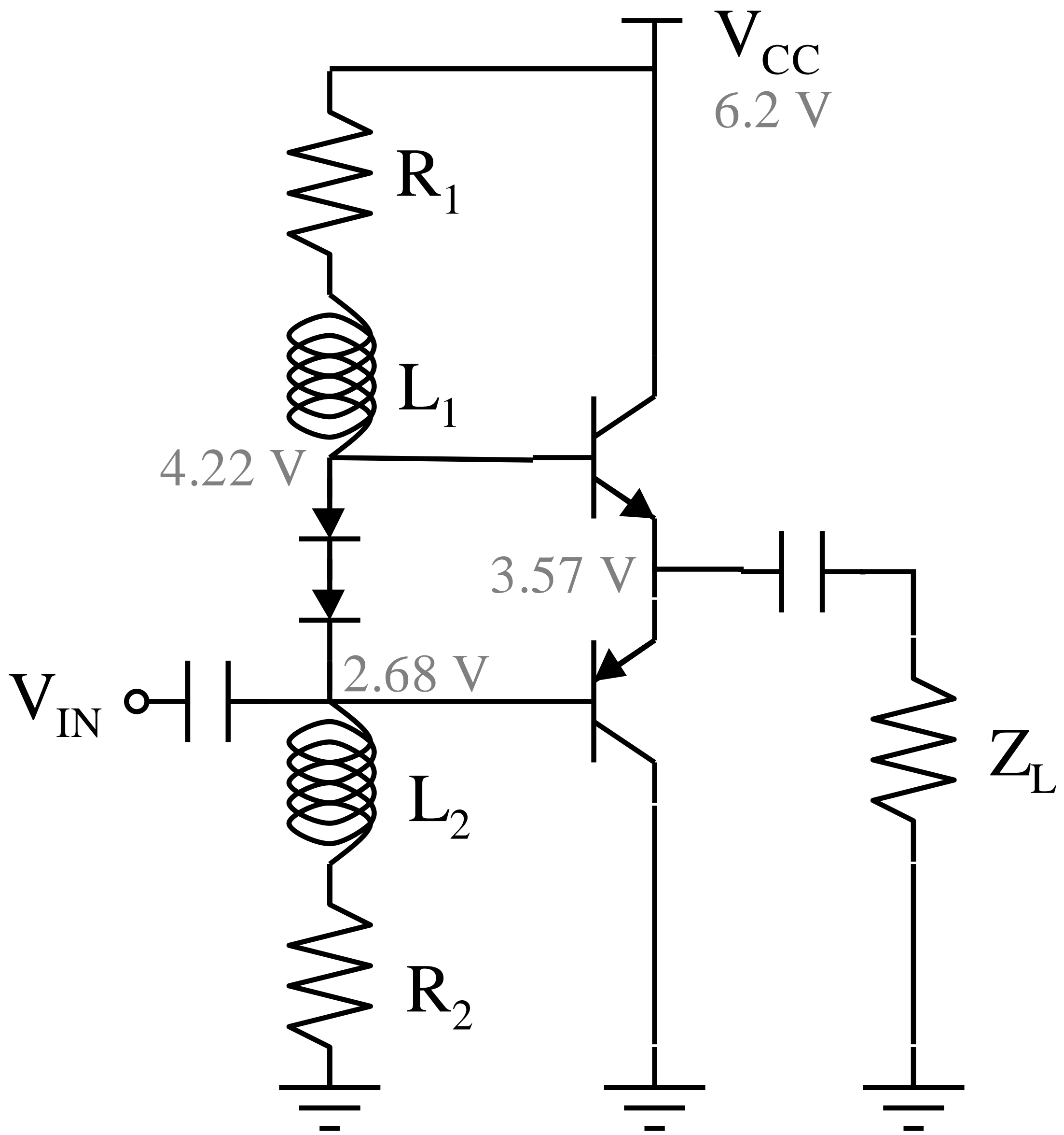

Figure 3

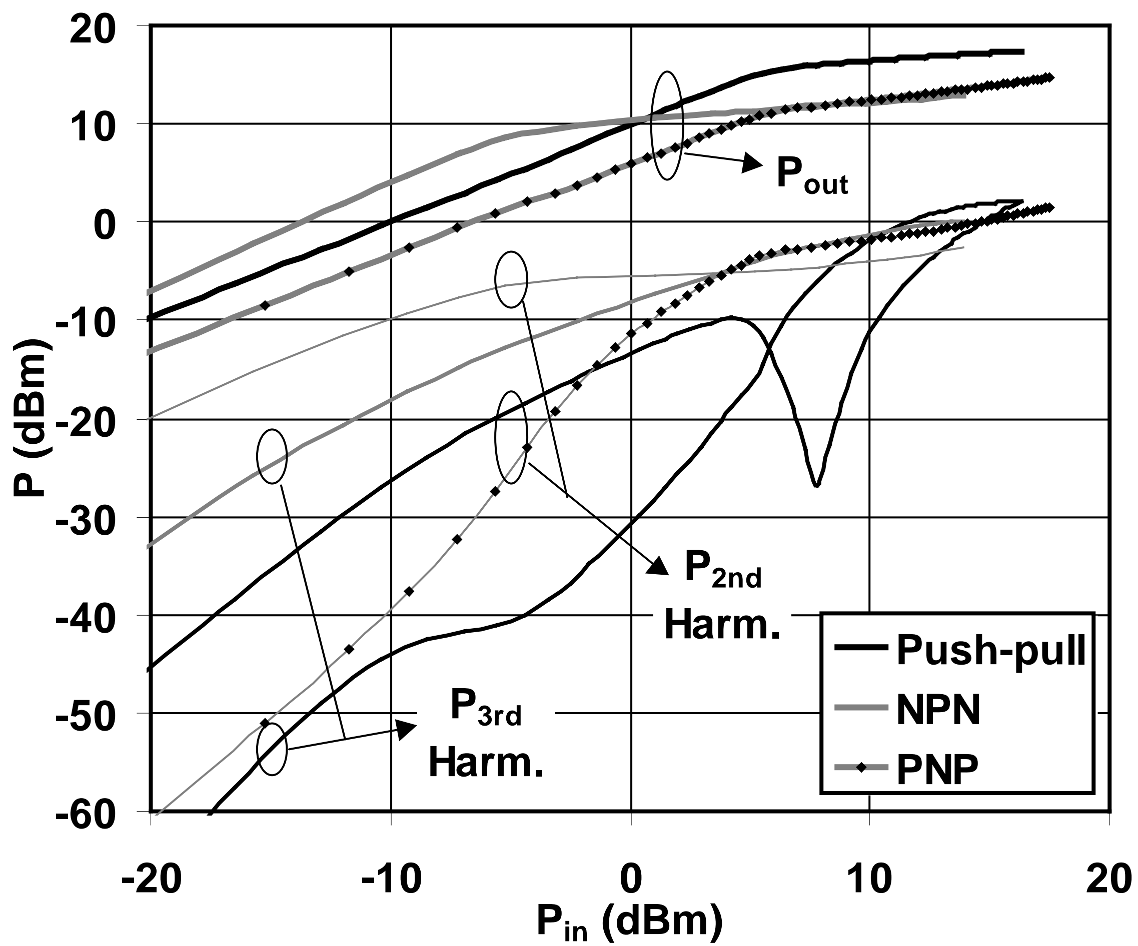

Figure 4

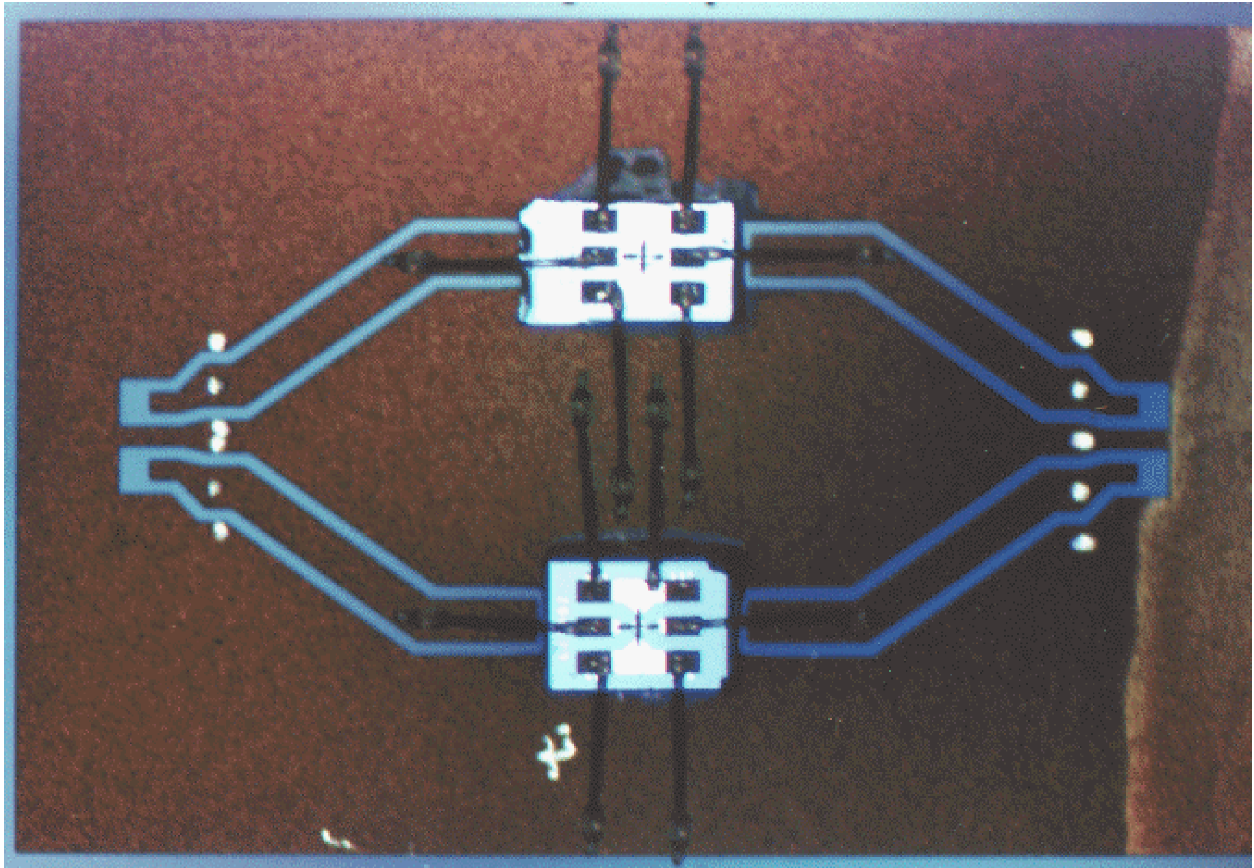

Figure 5

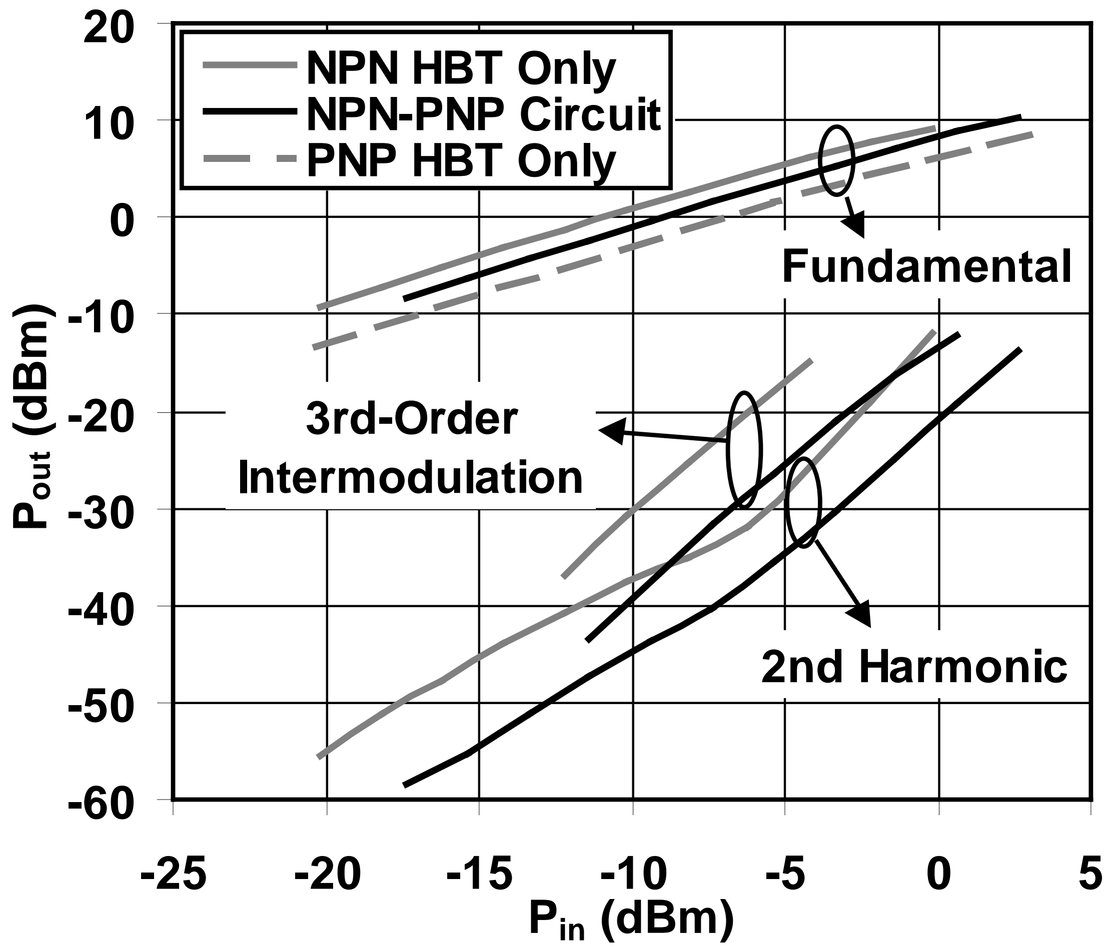

Figure 6